https://doi.org/10.5194/nhess-2020-128
Preprint. Discussion started: 25 May 2020

Natural Hazards and Earth System Sciences
Discussions

Evaluation of global seismicity along Northern and Southern hemispheres

Olaide Sakiru Hammed[1], Theophilus Aanuoluwa Adagunodo[2,*], Musa Oluwafemi Awoyemi[3], Joel Olayide Amosun[4], Tokunbo Sanmi Fagbemigun[4] and Tobi Ebenezer Komolafe[1]

[1]Department of Physics, Federal University, Oye-Ekiti, Nigeria
[2]Department of Physics, Covenant University, Ota, Nigeria
[3]Department of Physics, Obafemi Awolowo University, Ile-Ife, Nigeria
[4]Department of Geophysics, Federal University, Oye-Ekiti, Nigeria
* Corresponding author e-mail: taadagunodo@gmail; theophilus.adagunodo@covenantuniversity.edu.ng

Abstract

An earthquake has been identified as one of the major natural disasters that cause loss of lives and property. To mitigate this disaster, knowledge of global seismicity is essential. This research is aimed at evaluating the Gutenberg Richter b-value parameter and focal depth distribution of earthquake parameters to identify the prominent earthquake-prone zones in the Northern and Southern hemispheres. The study area covers 20° to the Northern and Southern hemispheres, with the equator in the middle. The data were obtained from the earthquake catalogue of the Advanced National Seismic System (ANSS) hosted by the Northern California Earthquake Data Centre USA from 1963 - 2018. Fifty-four-year earthquake data of $M \geq 6.0$ were processed and analyzed using Gutenberg-Richter (GR). The b-value parameters obtained from the GR model were plotted against the hemispheres using bar chart graphs to determine the tectonic stress level of the study region. The earthquake energy released was evaluated along the Northern and Southern hemispheres for a proper understanding of seismic events in the study region. It was observed that the rate of earthquake occurrence at the Southern hemisphere is higher than the Northern hemisphere. The b-values obtained in all the zones vary from 0.82 – 1.16. At the same time, the maximum earthquake energy of 4.6 × 1025 J was estimated. Low b-values indicate high tectonic stress within the plates. The large tectonic stress accumulation around the equator suggests that unstable lithospheres characterize this zone.

Keywords: b-value, Seismicity, Focal depth, Lithosphere, Equator, Earthquake energy

1. Introduction

The destruction associated with large earthquakes is one of the primary motivations for studying seismicity. The major concern about an earthquake is its radiative energy being released during its occurrence, which poses a threat to humankind. Proper investigation of the energy released by great earthquakes could proffer insights on the dynamics of the lithospheric plates. It has been established from previous studies on latitudinal variations of the energy released by earthquake events and its occurrence pattern that significant seismic events were observed to occur below latitudes ± 45° (Varga et al. 2012; Riguzzi et al. 2010; Levin and Sasorova, 2009; Dennis et al. 2002; Levin and Chirkov, 2001; Shanker et al. 2001; Varga, 1995; Sun, 1992; Chouhan and Das, 1971). The primary

https://doi.org/10.5194/nhess-2020-128
Preprint. Discussion started: 25 May 2020

mechanism that is associated with the release of energy at a deeper source is an earthquake (Kirby et al. 1991; Abe and Kanamori, 1979; Richter, 1979; Chouhan and Das, 1971). It has been documented that when these deep energies are released, they are not uniformly distributed along the earth's radius (Gutenberg and Richter 1956, 1954, 1942, 1936). About 25% of the global earthquakes occur at focal depth > 60 km (Frohlich, 2006), and of the total energy released, 0.2% came from foci earthquakes with depths > 300 km (deep focus) (Abe and Kanamori, 1979). The analysis of great earthquakes from seismically active zones showed that the earth is silent at depths beyond 680 km, and the deformations at these depths exist within the viscous regime (Abe and Kanamori, 1979). This study aims to determine the levels of tectonic stress accumulation along the Northern and Southern hemispheres to identify the regions that are likely prone to major earthquakes in the future.

2. Materials and methods

For this study, the data were extracted from the earthquake catalogue of the Advanced National Seismic System (ANSS) hosted by the Northern California Earthquake Data Centre U.S.A in a readable format. The data comprised earthquakes of $M \geq 6$ that occurred along the latitudinal boundary of 20° S to 20° N (Figure 1) from 1963 to 2018. The data comprised the date and time of occurrence, the latitude and longitude of the epicenter, the depth, the magnitude designation, source codes, and event identification. The data were sorted and filtered in preparation for further processing using the CompiCat software (Kossobokov et al. 2011). The study area, which is a strip of width 40^0 around the globe with the equator at the middle, was subdivided into four regions, each of 5^0 widths along the Northern and Southern hemispheres. The areas along the Northern hemisphere are: latitudes 0^o to 5^oN, 5^o to 10^oN, 10^o to 15^oN, and 15^o to 20^oN, while the regions along the Southern hemisphere are: latitudes 0^o to 5^oS, 5^o to 10^oS, 10^o to 15^oS, and 15^o to 20^oS, respectively.

https://doi.org/10.5194/nhess-2020-128
Preprint. Discussion started: 25 May 2020

Fig. 1: World map showing the latitudinal boundary of 20° S to 20° N (Adapted from MapsNworld, 2011).

The Gutenberg Richter (GR) relation parameter b-value was evaluated in order to establish the levels of tectonic stress accumulation along the northern and southern hemispheres (Adagunodo et al. 2018a; Hammed et al. 2016a; Nuannin, 2006; Damanik et al. 2010). GR relation is the frequency magnitude distribution that defines the total number of earthquake events in an area with respect to their magnitude (M). The GR model used is revealed in Equation (1).

$$\log N = a - bM \tag{1}$$

where N is the cumulative number of earthquakes with magnitudes equal to or greater than M, and a and b are real constants whose values vary in space and time.

An a-value represents the seismicity level, while the b-value corresponds to the slope of the power-law and describes the size distribution of events. A high b-value indicates a larger proportion of

https://doi.org/10.5194/nhess-2020-128
Preprint. Discussion started: 25 May 2020

Natural Hazards and Earth System Sciences
Discussions

small events and vice-versa. Also, the b-value represents the tectonic character of an area, which is a function of the accumulated stress within the lithospheric plates (Hammed et al. 2016a). These two parameters have been used in the tectonic analysis, earthquake prediction, seismic risk analysis, and seismicity study across the globe (Adagunodo et al. 2018b). As described by Hammed et al. (2016a), b-value, which is inversely dependent on the differential stress, and serves as an indicator of stress level, that is, a region with high-stress level often have relatively low b-value. The b-value of each section (that is, 5° divisions) within the study area is computed as a slope of the line of best fit. Besides, b-values are plotted against the hemispheres using bar chart graphs to understand the tectonic stress level of the study region.

The seismicity parameters such as earthquake energy, earthquake magnitude, earthquake focal depth, and earthquake epicenter were analyzed. As reported by Amiri et al. (2008), it is paramount to investigate the seismicity parameters in order to mitigate its effect in the future. For a proper understanding of the seismic activities in the study area, the energy released by an earthquake is plotted against its epicenter in the Northern and Southern hemispheres (Ghosh, 2007). The energy released, E, by an earthquake, can be estimated based on Gutenberg and Richter relations (Gutenberg and Richter, 1954; 1956), as shown in Equations 2 and 3.

$$\text{Log } E = 11.8 + 1.5 \text{ Ms (erg)} \quad (2)$$

$$\text{Log } E = 5.8 + 2.4 \text{ Mb (erg)} \quad (3)$$

where Mb and Ms are the body-wave and surface-wave magnitudes,

1 erg = 10^{-7} Joule (Hammed et al. 2016b).

The variation of earthquake focal depth with magnitudes in the hemispheres was plotted using 3D CompiCat plots to assess the seismic hazard along the hemisphere on a global scale. The temporal distribution of seismicity in the hemispheres was evaluated using frequency-time graph analysis.

3. Results and discussion

3.1 Trend of Seismicity and Tectonic characterization along the hemispheres

The degree of correlation coefficient (R^2) of the Gutenberg-Richter equations obtained for all latitudinal zones (Fig. 2 – 9) along the hemispheres is significant enough, due to its closeness to 1, to serve as a correlator. This implies that both the number of events and the corresponding magnitudes are much correlated. Thus, the Gutenberg -Richter b values of earthquakes obtained from this correlation are valid to be used as the tectonic stress accumulation indicator along the hemispheres.

The b-value is the stress meter that indicates the level of tectonic stress accumulation in the earthquake-prone zones, Hammed et al. (2019). The lower the b-value, the higher the tectonic stress and vice-versa (Awoyemi et al. 2017; Hammed et al. 2013). In this work, the b values obtained in all

https://doi.org/10.5194/nhess-2020-128
Preprint. Discussion started: 25 May 2020

Natural Hazards and Earth System Sciences
Open Access
Discussions

the zones vary from 0.82 – 1.16, as shown in Fig. 2 - 9. Along the Northern and Southern Hemispheres, the latitude zones 0 - 5N and 0 - 5S that is 10^o across the equator are characterized by very low b values (Fig. 10). The implication of the low b values associated with these zones is that the zones are embedded with large tectonic stress accumulation. Thus, there is a strong plausibility that the zones may be prone to disastrous earthquakes in the future.

The analysis of the trend of seismicity along the hemispheres revealed that the rate of earthquake occurrence in the Southern Hemisphere is higher than that of the Northern Hemisphere (Fig. 11). This implies that the phenomena that are associated with seismicity, such as the rate of divergence and convergence of lithospheric plates, are higher in the southern part of the equator. The seismicity is heavily distributed around the equatorial region at -5^o to $+5^o$ (Fig. 12). This further confirms that the high rate of tectonic stress accumulation around the equator is indicated by low b-values.

The weighted sum of earthquake energy counts along the hemispheres is densely distributed in the equatorial region (Fig. 12). At latitude -5^o to $+5^o$, it is observed that the earthquake energy increased significantly up to the peak of 5.4×10^{24} J. This is an indication that the equatorial regions are characterized by large tectonic stress accumulation which implies that the lithospheric layers in these regions are very unstable.

3.2 Distributions of focal depth, frequency, and energy of earthquake released

The focal depth distributions (70 km depth classes) of the number of events (frequency) and energy of earthquakes are shown in Fig. 13 and 14, respectively. The number of events decreases with an increase in focal depth up to about 300 km. From 300 to 500 km, the numbers of events are sparse and sporadic. This zone could be interpreted as a subduction zone (Riguzzi 2010). Beyond this focal depth range, there is a significant increase in the number of events up to 700 km. Most of the elastic energy radiated by deep events are concentrated in the depth interval between 500 km and 700 km. In summary, 94.16% of the events occur within 300 km, while the remaining 5.84% occur from 300 to 700 km. About 77.38% of the total number of earthquakes is concentrated in the first depth class (0–70 km); 16.71% occur from 70 to 300 km; the remaining 5.92% up to 700 km. As regards to the earthquake energy, 85% is dissipated within 300 km, the remaining 15% from 300 to 700 km, where most of the energy dissipation is viscous. About 70% of the total amount of energy is concentrated in the first depth range (0–70 km), with maximum sharp energy of approximately 4.6×10^{25} J; 15% is dissipated from 70 to 300 km, and the remaining 15% up to 700 km. Only 5.92% of all the earthquakes released accounts for about 15% of the total energy release at depth 500–700 km. The deep event clustering is marked by high energy release (energy peak ~ 0.2×10^{25} J).

The predominant clustering of magnitudes M6+ within the shallow focal depth (< 100 km) along the hemispheres (Fig. 15) indicates a high level of stress in the lithosphere around the equator. The

https://doi.org/10.5194/nhess-2020-128
Preprint. Discussion started: 25 May 2020

maximum energy of about 4.6×10^{25} J generated at shallow depth within this zone suggests that this zone is characterized by unstable lithosphere.

3.3 Temporal distribution of seismicity along the hemispheres

The analysis of the temporal distribution of seismicity along the hemispheres (Fig. 16) revealed that the earthquakes increase with time, and decade wise. The earthquakes are densely distributed around the equator in the last three decades. The increase and densely distribution of earthquakes along the equatorial zones is an indication that the lithospheric layer embedded in this zone is not as stable as early thought. This deviation could have been due to improved monitoring of the equatorial region. The increase in tectonic stress accumulation around the hemispheres could trigger continuous occurrences of an earthquake.

https://doi.org/10.5194/nhess-2020-128
Preprint. Discussion started: 25 May 2020

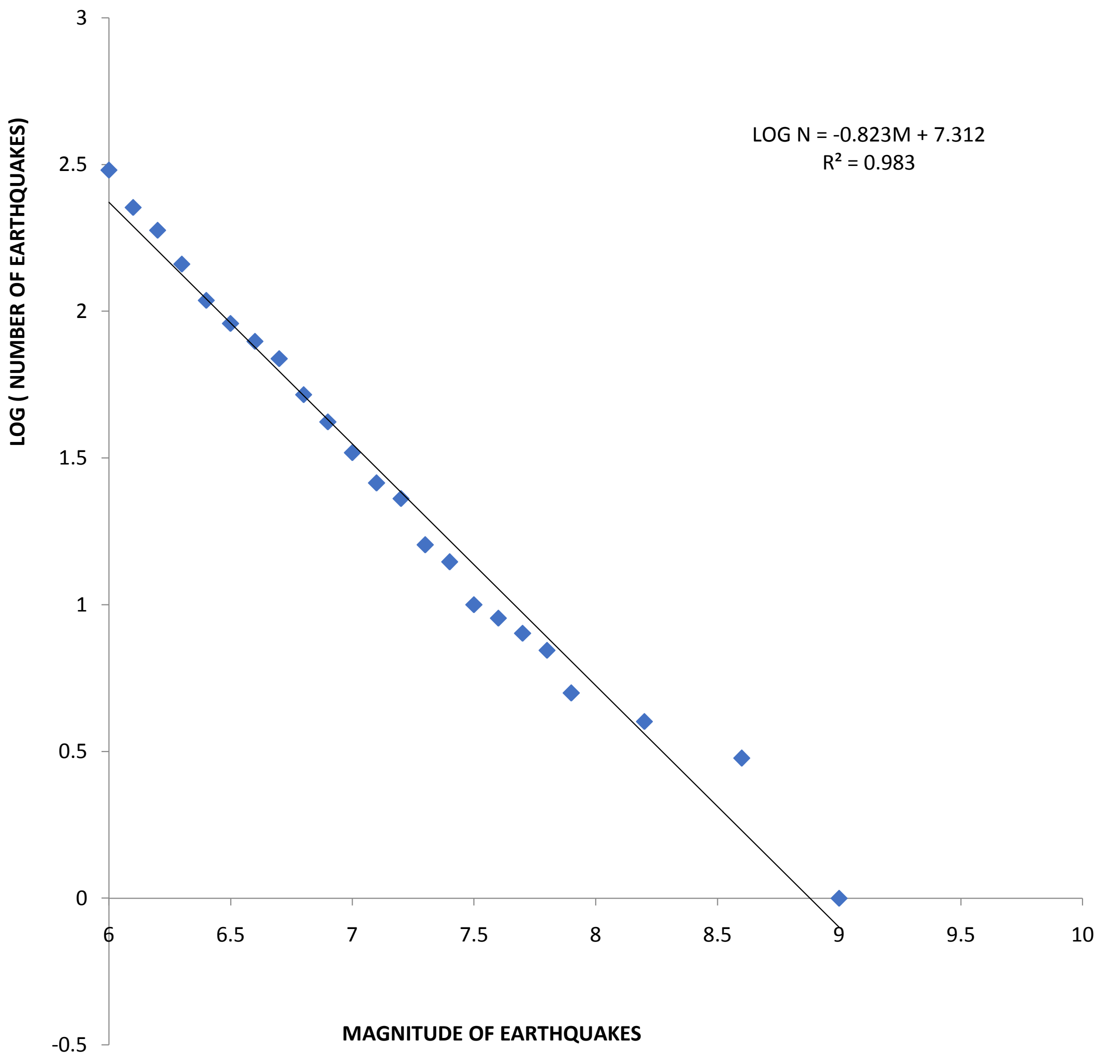

161

162 Fig. 2 Frequency Magnitude Distribution of Earthquakes along Northern Hemisphere 0^o – 5^{o}N

https://doi.org/10.5194/nhess-2020-128
Preprint. Discussion started: 25 May 2020

Natural Hazards and Earth System Sciences
Open Access
EGU
Discussions

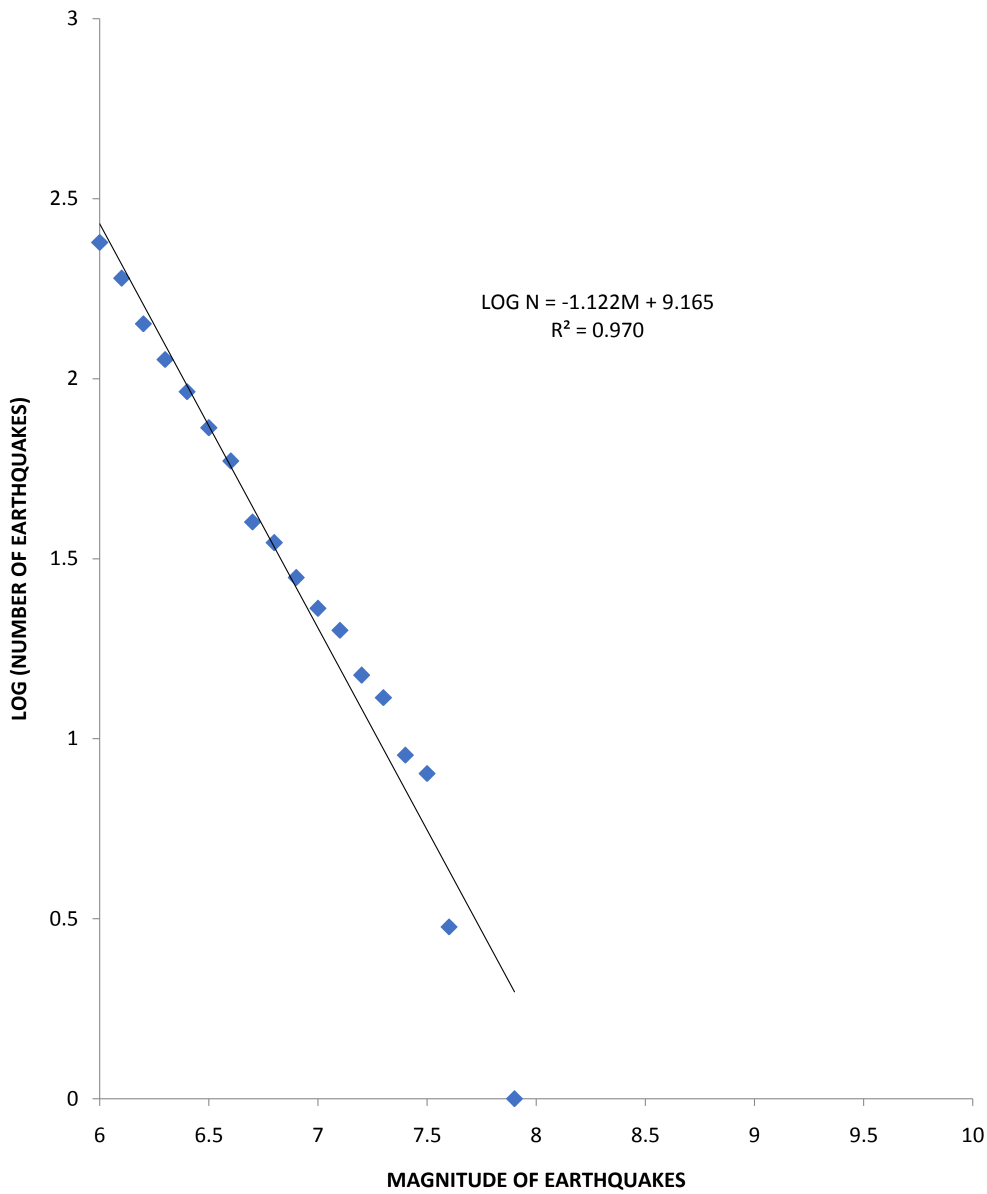

163

164 Fig. 3 Frequency Magnitude Distribution of Earthquakes along Northern hemisphere5^{o} – 10^{o}N

https://doi.org/10.5194/nhess-2020-128
Preprint. Discussion started: 25 May 2020

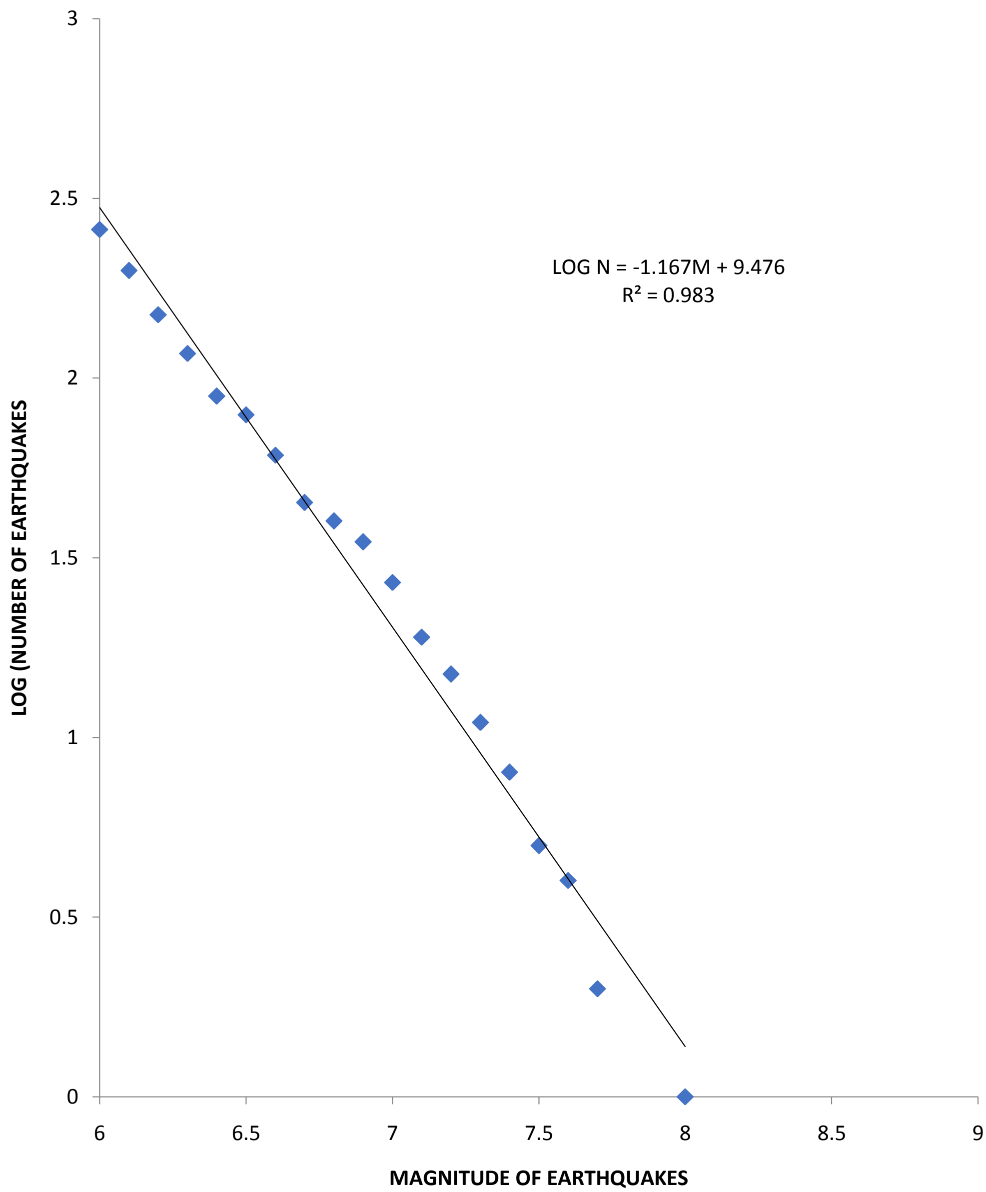

Fig. 4 Frequency Magnitude Distribution of Earthquakes along Northern Hemisphere 10^{o} – 15^{o}N

https://doi.org/10.5194/nhess-2020-128
Preprint. Discussion started: 25 May 2020

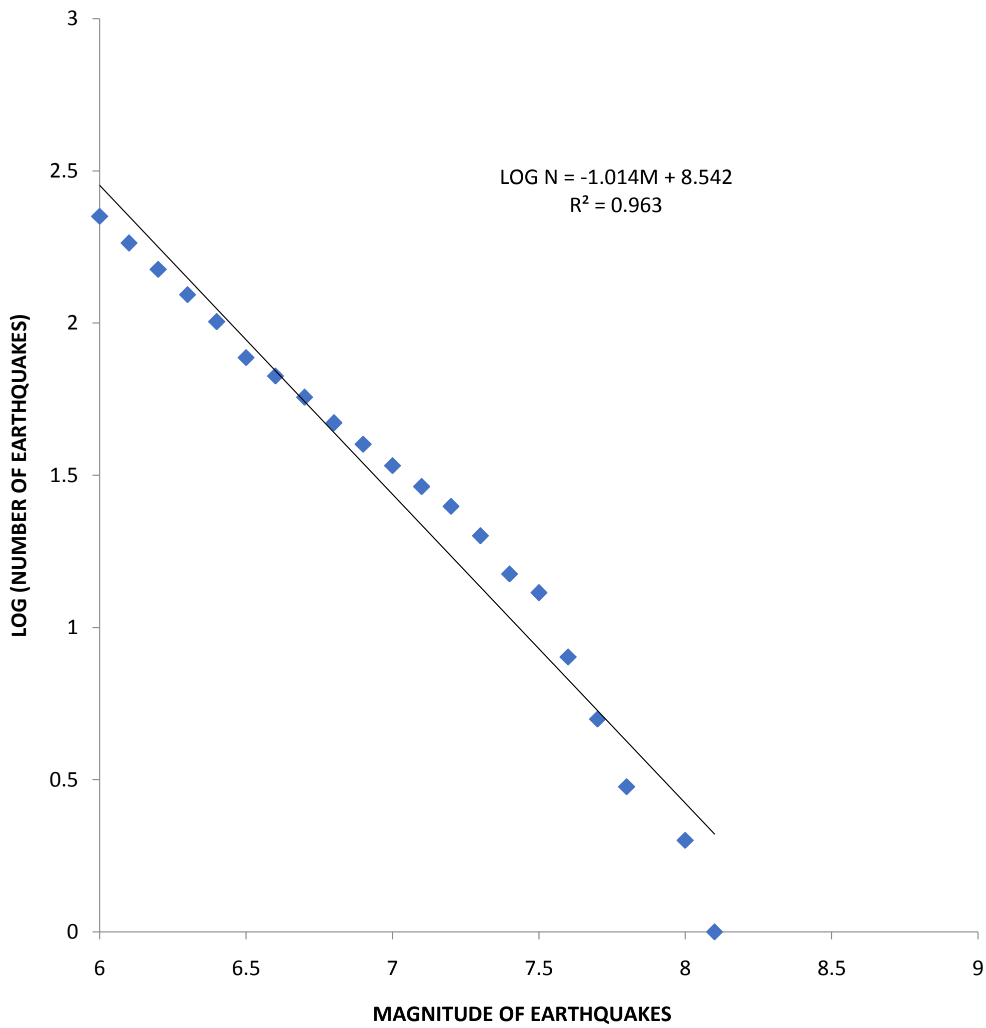

Fig. 5 Frequency Magnitude Distribution of Earthquakes along Northern Hemisphere 15^o – 20^{o}N

https://doi.org/10.5194/nhess-2020-128
Preprint. Discussion started: 25 May 2020

Natural Hazards and Earth System Sciences
Open Access
Discussions

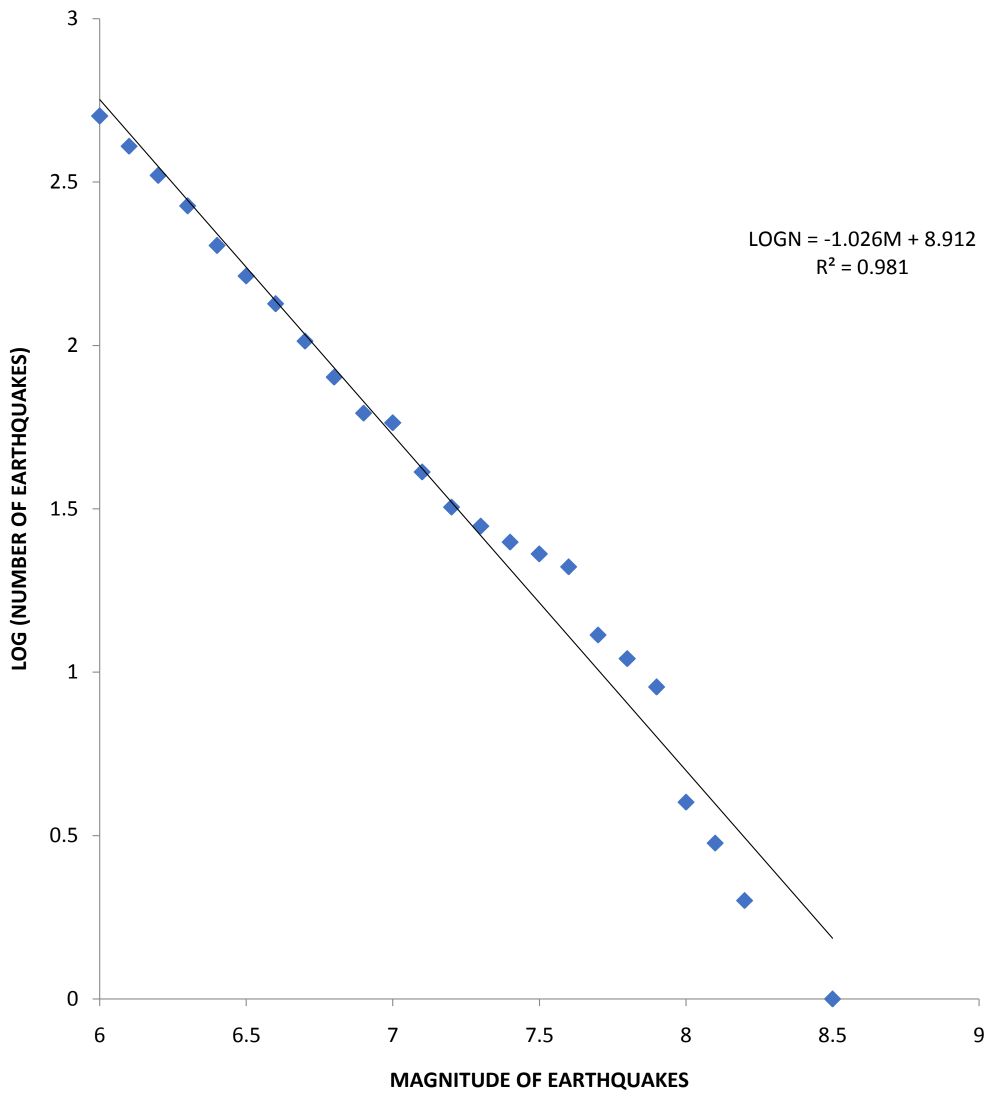

Fig. 6 Frequency Magnitude Distribution of Earthquakes along Southern Hemisphere $0^o – 5^o$S

https://doi.org/10.5194/nhess-2020-128
Preprint. Discussion started: 25 May 2020

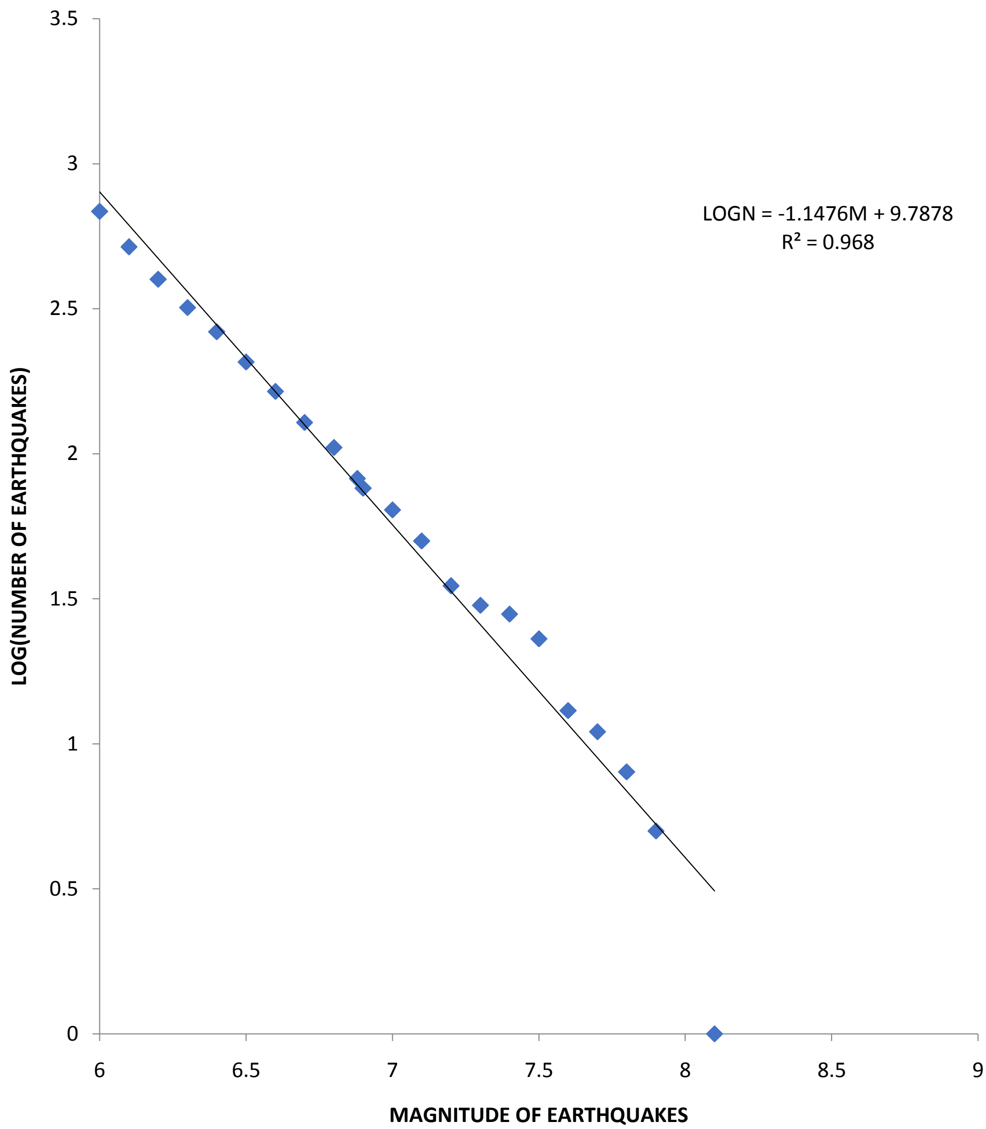

Fig. 7 Frequency Magnitude Distribution of Earthquakes along Southern Hemisphere $5^o – 10^o$S

https://doi.org/10.5194/nhess-2020-128
Preprint. Discussion started: 25 May 2020

Natural Hazards and Earth System Sciences
Open Access
Discussions

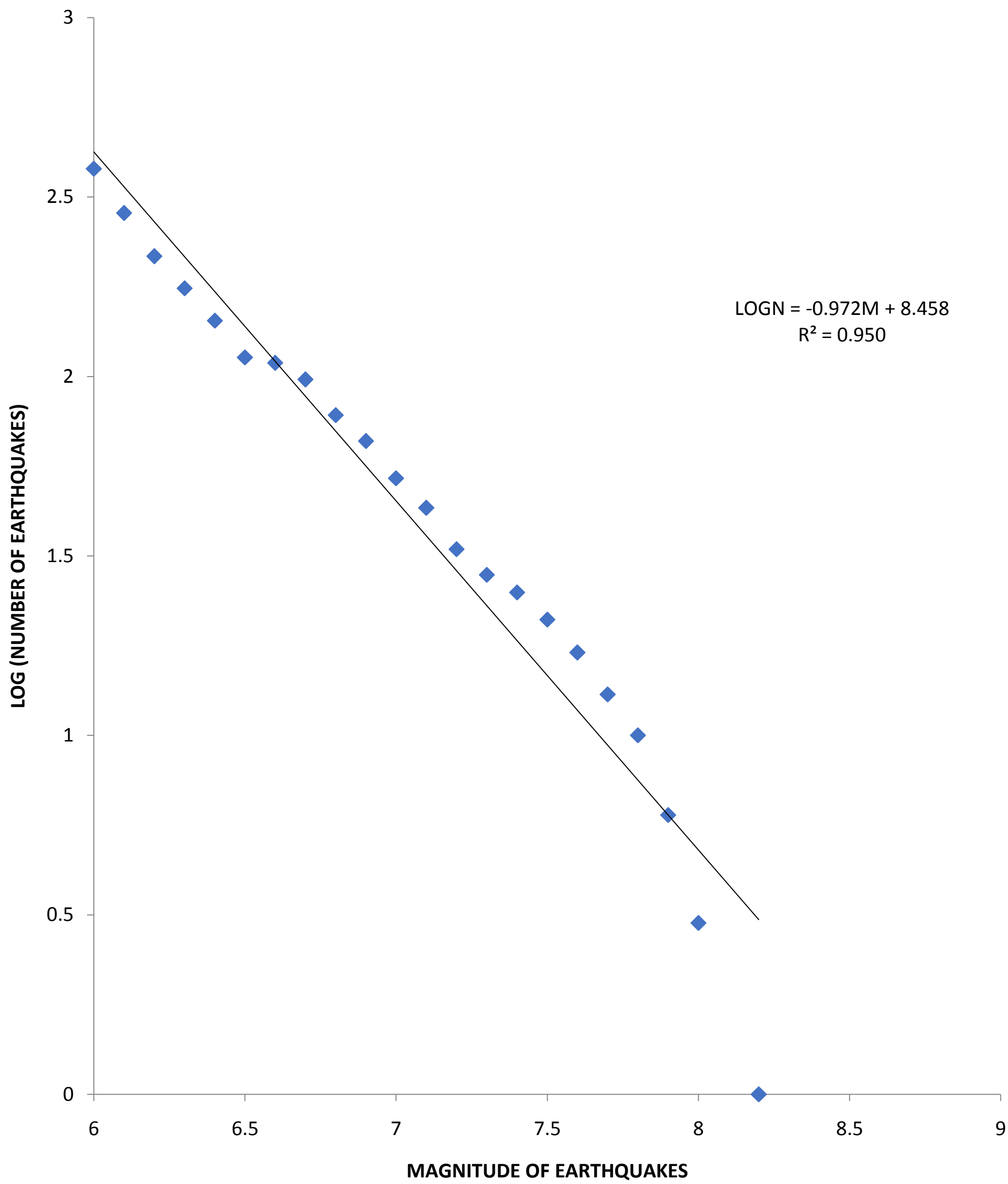

Fig. 8 Frequency Magnitude Distribution of Earthquakes along Southern Hemisphere 10^{o} – 15^{o}S

https://doi.org/10.5194/nhess-2020-128
Preprint. Discussion started: 25 May 2020

Natural Hazards and Earth System Sciences Discussions

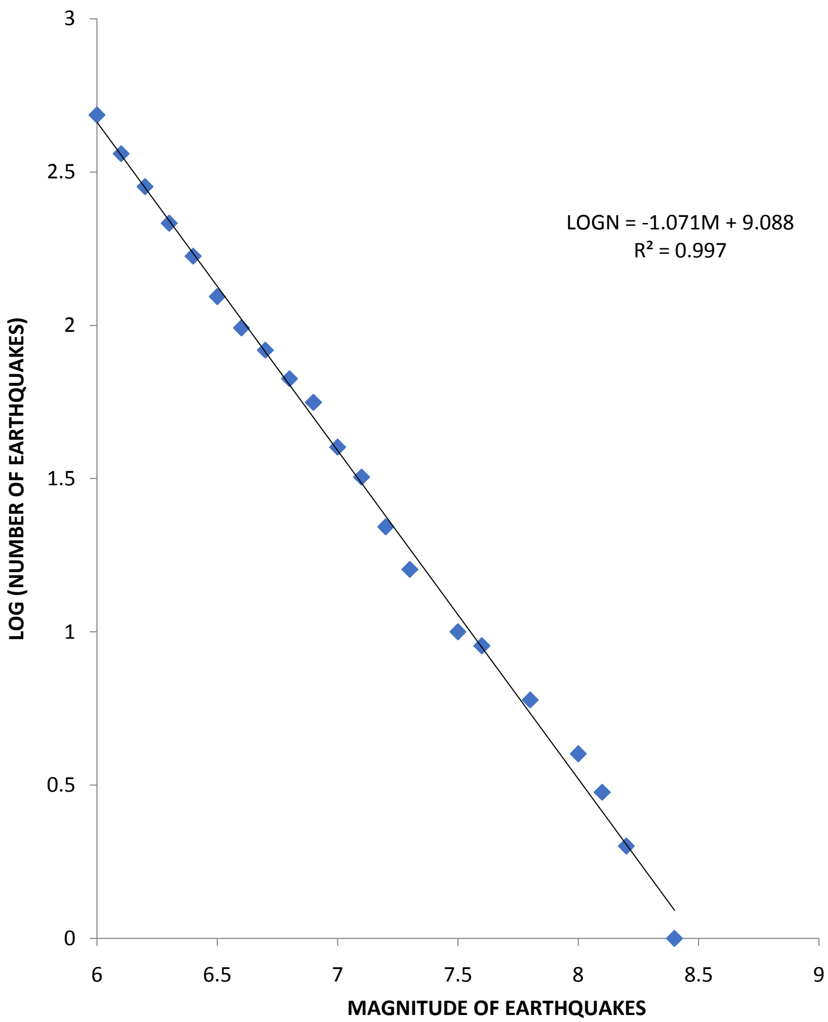

Fig. 9 Frequency Magnitude Distribution of Earthquakes along Southern Hemisphere 15° – 20°S

https://doi.org/10.5194/nhess-2020-128
Preprint. Discussion started: 25 May 2020

Natural Hazards and Earth System Sciences
Open Access
Discussions

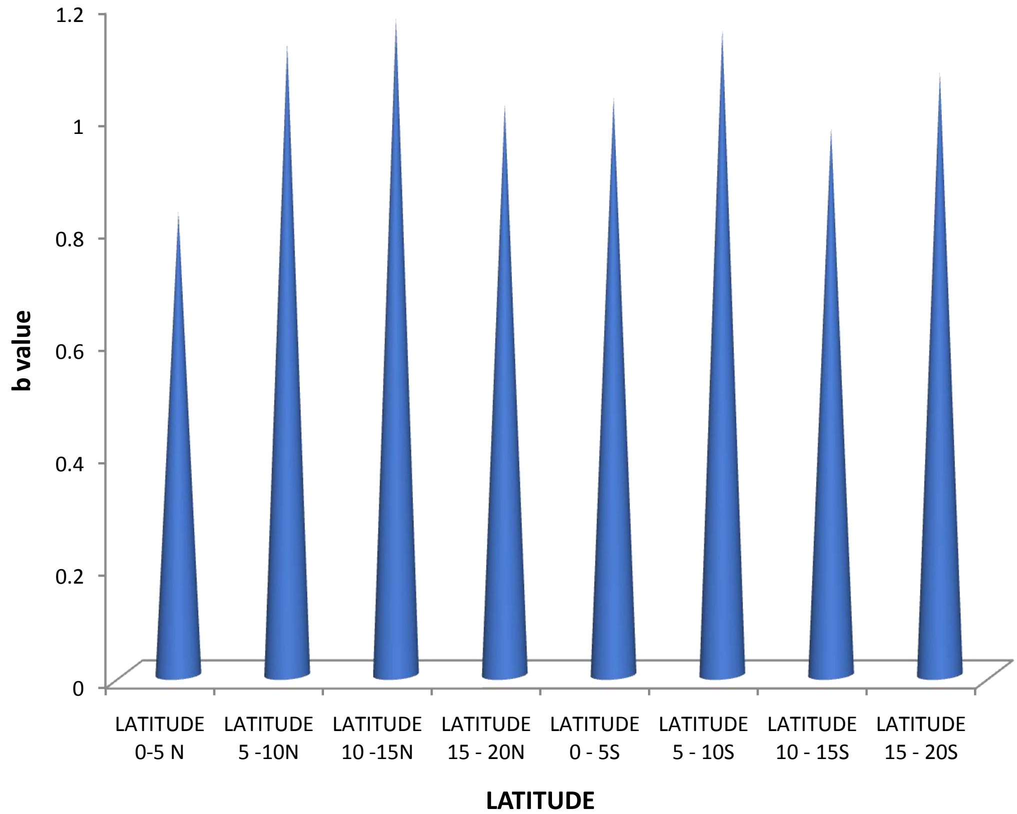

Fig. 10 Distribution of b-value along Northern and Southern Hemisphere

https://doi.org/10.5194/nhess-2020-128
Preprint. Discussion started: 25 May 2020

Natural Hazards and Earth System Sciences
Discussions

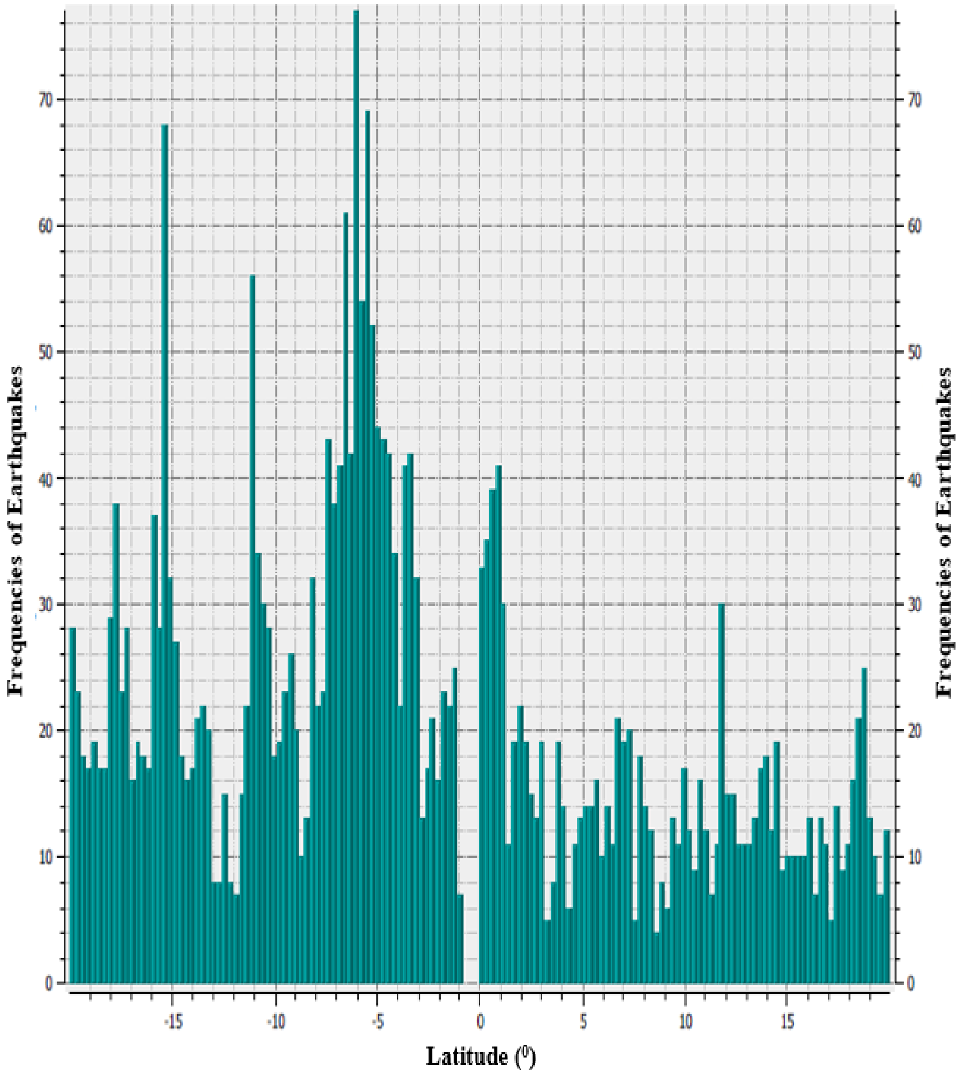

Fig. 11 Distribution of frequency of earthquakes along Northern and Southern Hemisphere

https://doi.org/10.5194/nhess-2020-128
Preprint. Discussion started: 25 May 2020

Natural Hazards and Earth System Sciences
Discussions

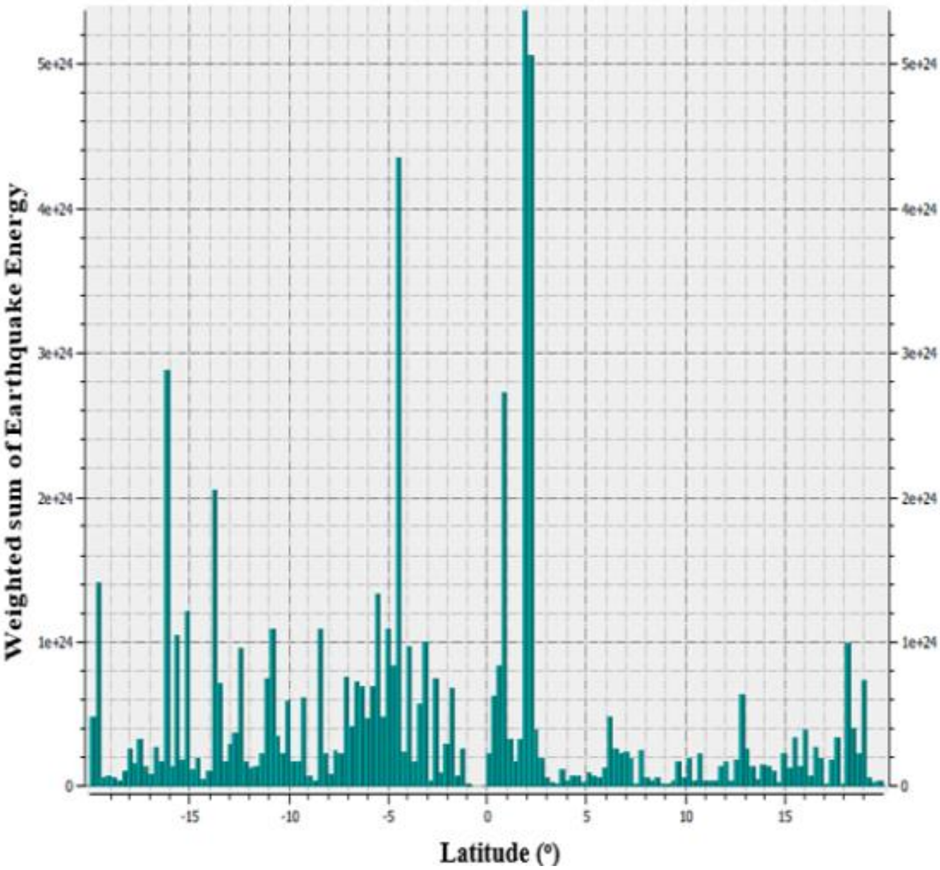

Fig. 12 Distribution of Weighted Sum of Earthquake Energy along Northern and Southern Hemispheres

https://doi.org/10.5194/nhess-2020-128
Preprint. Discussion started: 25 May 2020

Natural Hazards and Earth System Sciences
Open Access
EGU
Discussions

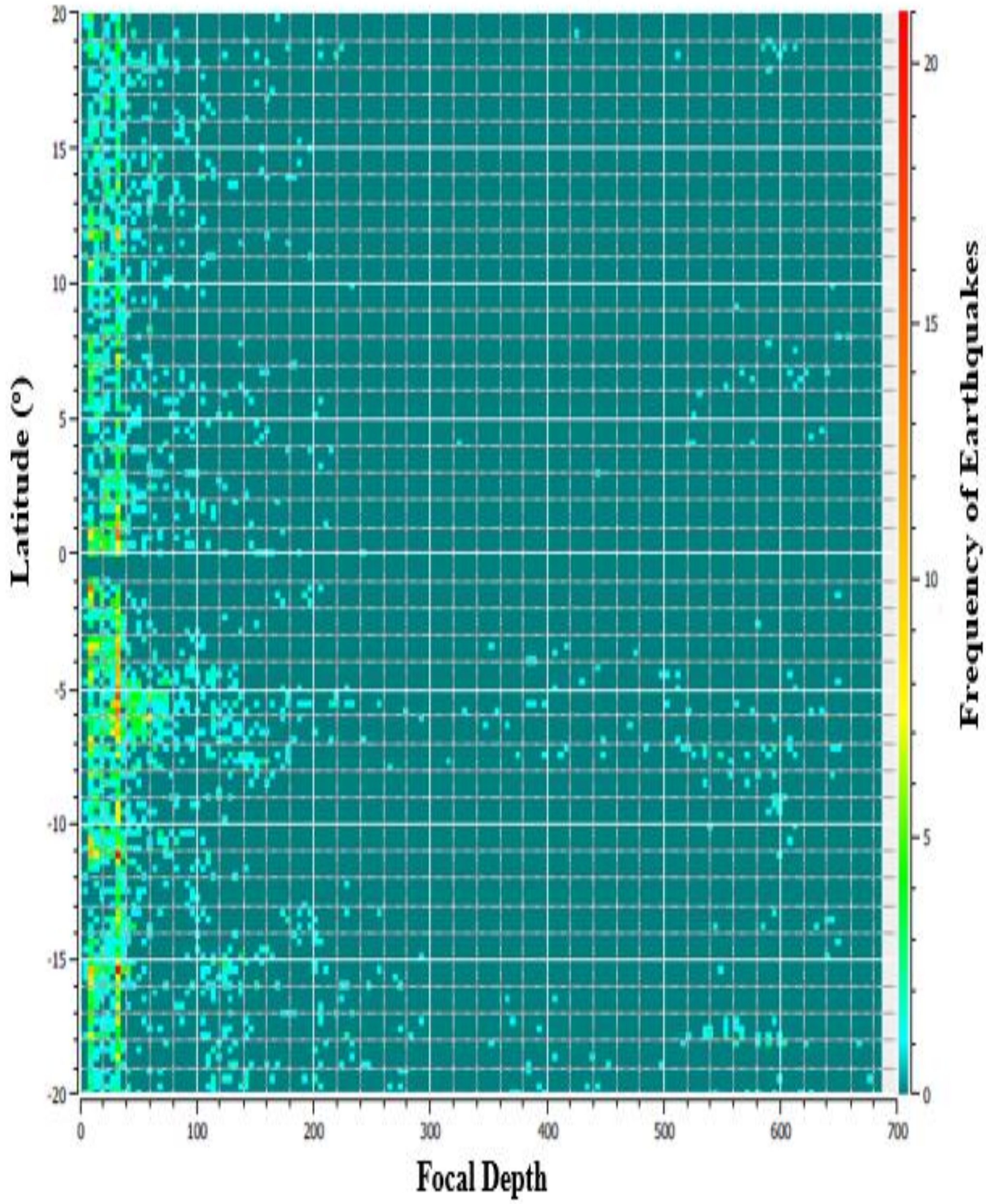

Fig. 13a 3D Focal depth distribution of Frequency of Earthquakes along the Latitudinal Zones

https://doi.org/10.5194/nhess-2020-128
Preprint. Discussion started: 25 May 2020

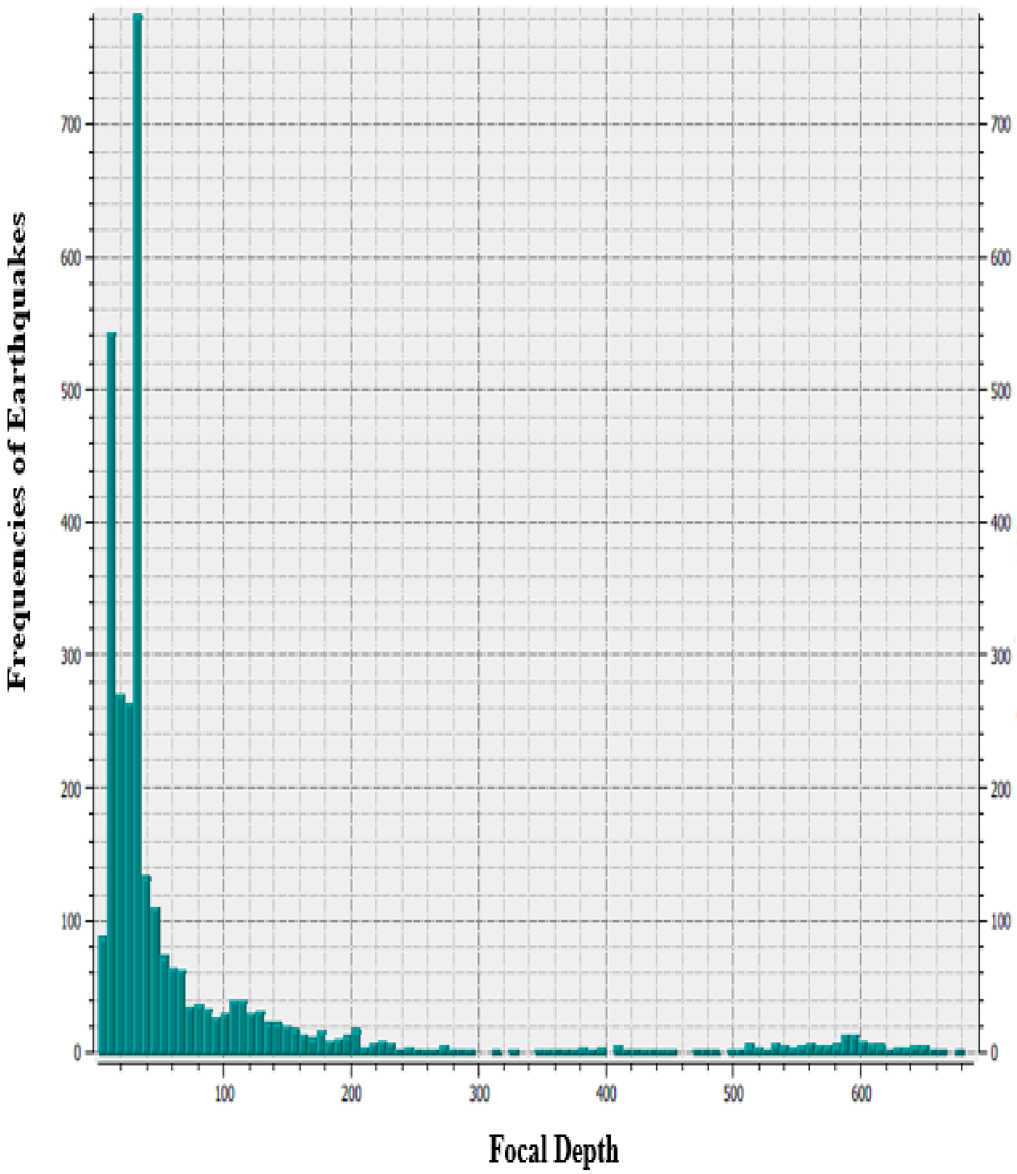

Fig. 13b Focal depth distribution of Earthquake Frequencies along the Northern and Southern Hemispheres

Natural Hazards and Earth System Sciences
Open Access
Discussions

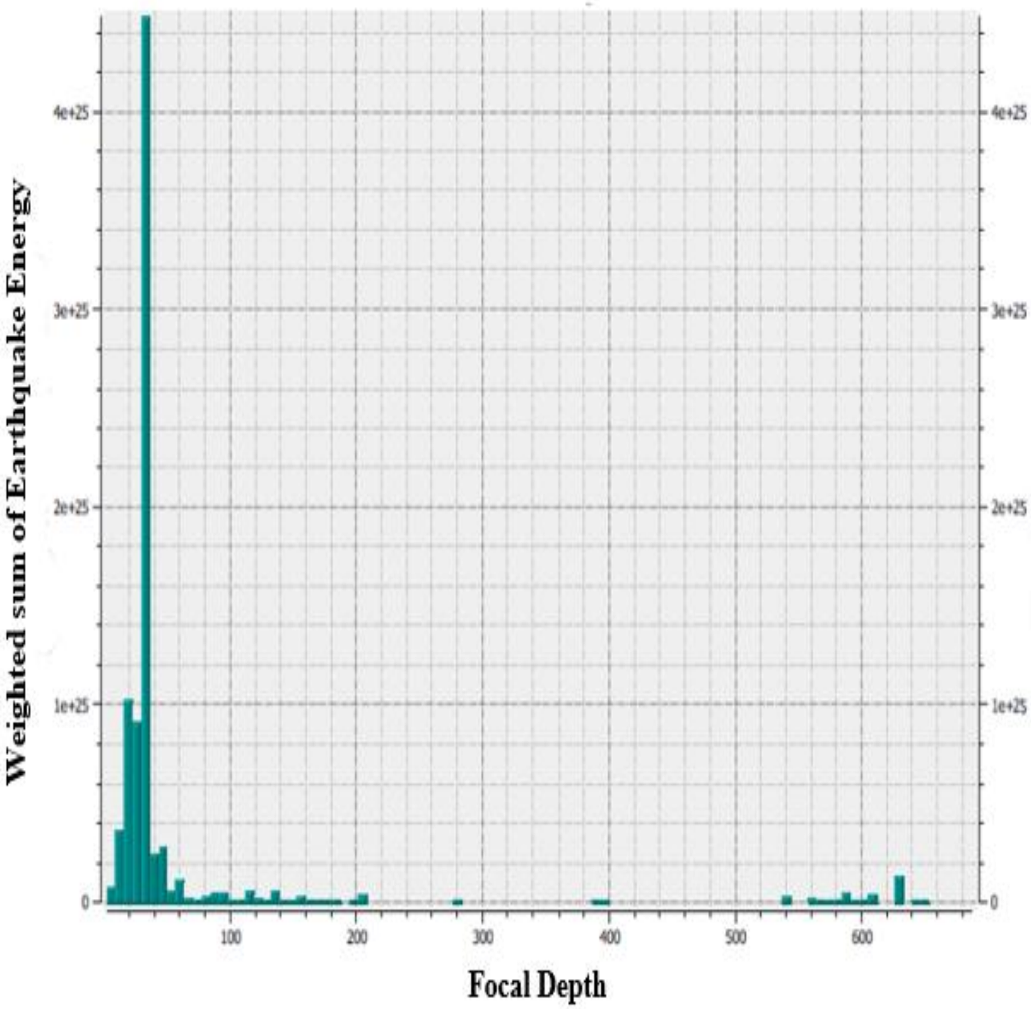

Fig 14 Focal depth distribution of weighted sum of Earthquake Energy along the Northern and Southern hemispheres

https://doi.org/10.5194/nhess-2020-128
Preprint. Discussion started: 25 May 2020

Natural Hazards and Earth System Sciences
Discussions

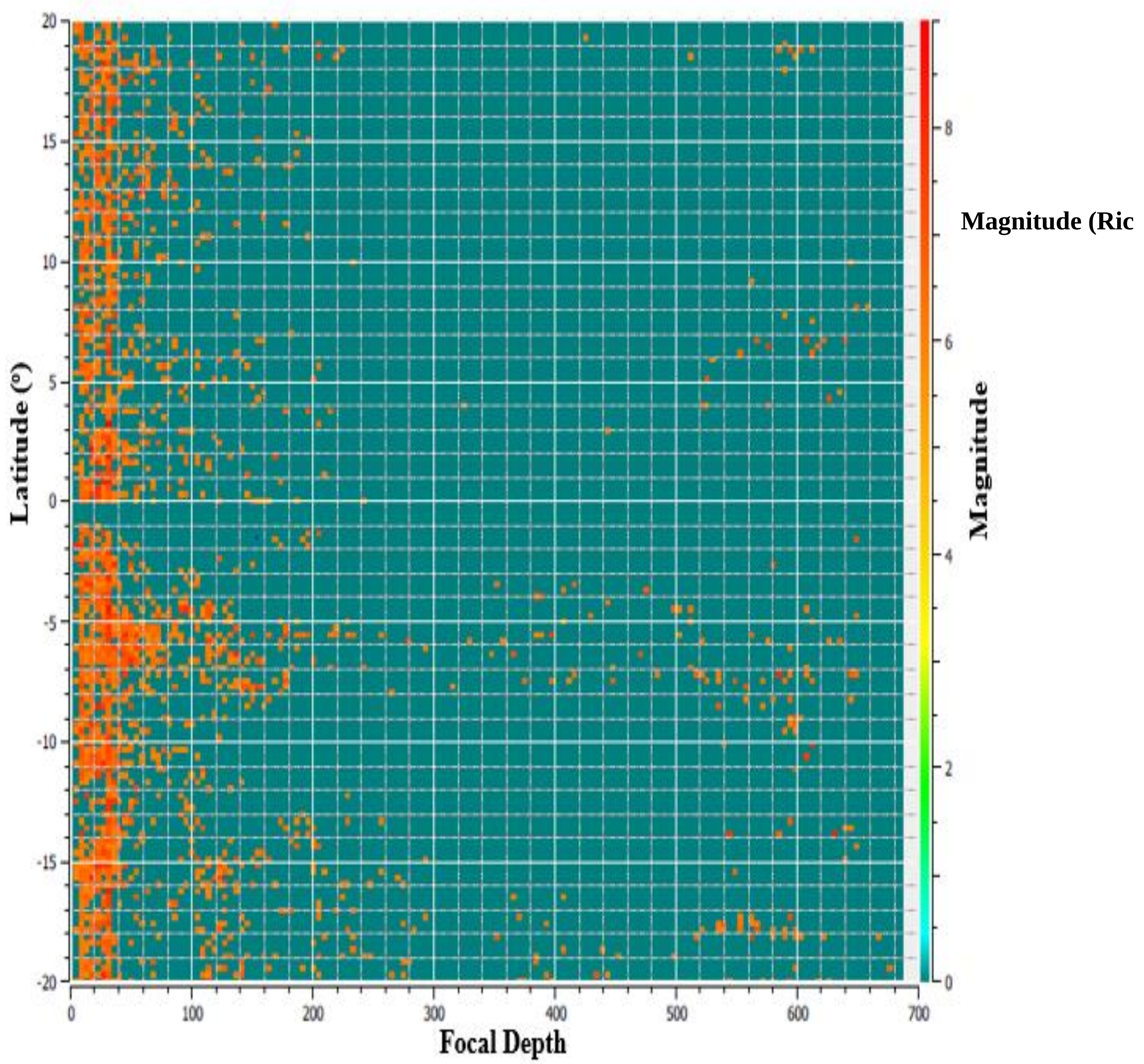

Fig 15 Focal depth distribution of magnitudes along the Northern and Southern Hemispheres

https://doi.org/10.5194/nhess-2020-128
Preprint. Discussion started: 25 May 2020

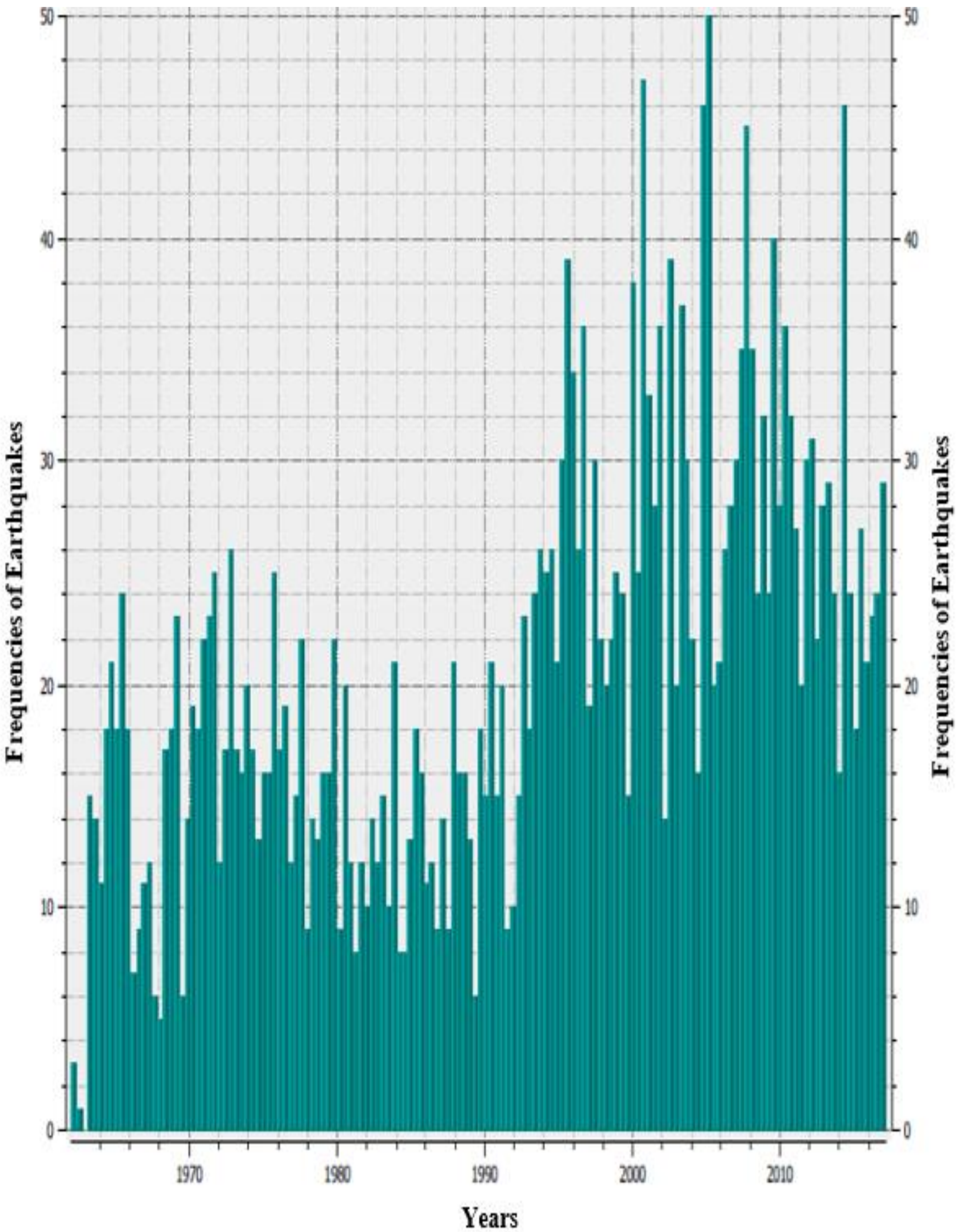

Fig. 16 Temporal variation of frequency of Earthquakes along Northern and Southern Hemispheres

4. Conclusion

The trend of seismicity along the hemispheres revealed that the rate of earthquake occurrence in the Southern hemisphere is higher than that of the Northern hemisphere. The b-values obtained from this study vary from 0.82 to 1.16. Very low b-values dominated the equatorial region, that is, 5° S to 5° N. This indicates that the level of stress around the equator is relatively high. The maximum earthquake energy of about 4.6×10^{25} J was estimated. 70% of the total amounts of energy calculated are housed in the shallow depth, while the intermediate and deep depths share 15% each. The shallow and the deep depths constitute the seismicity regime, as the numbers of events in the intermediate depth are scarce. To further evaluate the number of energies being hosted around the equator, 5° S to 5° N, a maximum of 5.4×10^{24} J of earthquake energy was estimated. This indicates that the equatorial regions are characterized by large tectonic stress accumulation. It can be concluded that the lithospheric plates around the equator are unstable. The temporal distribution of seismicity along the hemispheres revealed that the earthquakes increase with time, and decade wise. There is a strong plausibility that the regions around the equator may be prone to disastrous earthquakes in the future.

Author contribution

OSH, TAA and TEK conceived the study. OSH, TAA and MOA supervised the work. OSH, TAA, MOA, JOA and TSF processed, and anlyzed the data. TEK wrote the first draft. OSH and TAA revised, edited, and searched for the literature to produce the second and final draft. OSH, TAA, MOA, JOA, TSF and TEK gave technical supprot to improve the quality of the paper, read and approved the final draft for submission.

Competing Interests

We declare that there is no conflict of interest as regards this article.

REFERENCES

Abe K., Kanamori H. (1979). Temporal variation of the activity of intermediate and deep focus Earthquakes. *Journal of Geophysical Research*, **84,** 3589–3595.

Adagunodo T.A., Lüning S., Adeleke A.M., Omidiora J.O., Aizebeokhai A.P., Oyeyemi K.D., Hammed O.S. (2018a). Evaluation of 0 ≤ M ≤ 8 Earthquake Data Sets in African-Asian Region during 1966 – 2015. *Data in Brief*, **17C**, 588 – 603. https://doi.org/10.1016/j.dib.2018.01.049.

Adagunodo T.A., Oyeyemi K.D., Hammed O.S., Bansal A.R., Omidiora J.O., Pararas-Carayannis G. (2018b). Seismicity Anomalies of M 5.0 + Earthquakes in Chile during 1965 – 2015. Science of Tsunami Hazards, 37(2): 130 – 156.

Amiri G.G., Razeghi H.R., Razavian AmreiS. A., Aalaee H., Rasouli S.M. (2008). Seismic Hazard Assessment of Shiraz. *Iran Journal of Applied Sciences*, **8**, 38-48.

Awoyemi M.O., Hammed O.S., Shode O.H., Olurin O.T., Igboama W.N., Fatoba J.O. (2017). Investigation of b-value variations in the African and parts of Eurasian plates. Journal of Tsunami Society International, **36**(2), 86 – 99.

Chouhan R.K.S., Da, U.C. (1971). Preliminary report on global seismicity-frequency energy distribution of earthquakes. *Pure and Applied Geophysics* **89** (1), 98–108.

Damanik R., Andriansyah Putra, H. K., Zen M. T. (2010). Variations of b-values in the Indian Ocean– Australian Plate Subduction in South Java Sea. "Proceedings of the Bali 2010 International Geosciences Conference and Exposition, Bali, Indonesia", 19 – 22.

Denis C., Schreider, A.A., Varga, P., Závoti, J. (2002). Despinning of the Earth rotation in the geological past and geomagnetic paleointensities. *Journal of Geodynamics* **34** (5), 97–115.

Frohlich C. (2006). Deep Earthquakes. Cambridge University Press.

Ghosh A. (2007). Earthquake frequency-magnitude distribution and interface locking at the middle America subduction zone near Nicoya Peninsula Costa Rica Georgia institute of technology. http://smartech.gatech.edu/handle/ 1853/16288.

Gutenberg B., Richter C.F. (1936). Materials for the study of deep-focus earthquakes. *Bulletin of the Seismological Society of America* **26** (4), 341–390.

Gutenberg B., Richter C.F. (1942). Earthquake magnitude, intensity, energy, and acceleration. *Bulletin of the Seismological Society of America* **32**, 163–191.

Gutenberg B., Richter C.F. (1954). Seismicity of the Earth, 2nd edition. Princeton University Press.

Gutenberg B., Richter C.F. (1956). Earthquake magnitude, intensity, energy and acceleration (second paper). *Bulletin of the Seismological Society of America* **46,** 105–145.

Hammed O.S., Popoola O.I., Adetoyinbo A.A., Awoyemi M.O., Badmus G.O., Ohwo O.B. (2013). Focal depth, magnitude, and frequency distribution of earthquakes along Oceanic Trenches. *Earthquake Science*, **26**, 75 – 82.

Hammed O. S., Awoyemi M.O., Igboama W.N., Badmus G.O. and Essien U. C. (2016a). "Pattern of Seismicity Associated with the African Lithospheric Plate". *Physical Science International Journal*, **10** (3), 1-11.

Hammed O.S., Awoyemi M.O., Badmus G.O., Sanni O.O. (2016). Interdependence and Variations of Earthquake Parameters on African Lithospheric Plate using Getenberg and Richter Relation. Journal of Geography, Environment and Earth Science International, 4(4): 1-12.

Hammed O. S., Adagunodo T. A., Awoyemi M.O., Arogundade A.B., Ajama O.D., F.O. Sapele, Usikalu F.O., Olanrewaju M.R., Akinwunmi S. A.,Ogunwale E.I. (2019). Identification of tsunamigenic earthquake zones in oceanic ridges and trenches. *Science of tsunami hazards*. **38** (2), 103 -117.

Kirby S.H., Durham W.B., Stern L.A., (1991). Mantle phase changes and deep earthquake faulting in subducting lithosphere. *Science* , **252**, 216–225.

Kossobokov V., Mostinskiy A., Shebalin P. (2011). CompiCat Program. CompiCat Program Manual. Advanced School on Understanding and Prediction of Earthquakes and other Extreme Events in Complex System, September 26 to October 28, 2011. Pp 49.

Levin B.W., Chirkov Ye.B. (2001). Planetary maxima of the earth seismicity. *Physics and Chemistry of the Earth*, Part **C 26** (10–12), 781–786.

Levin B.W., Sasorova E.V. (2009). Latitudinal distribution of earthquakes in the Andes and its Peculiarity". *Advances in Geosciences* **22**, 139–145.

MapsNworld (2011). World Wall Map. Retrieved from https://www.mapsnworld.com/wall-map-of-world.html

https://doi.org/10.5194/nhess-2020-128
Preprint. Discussion started: 25 May 2020

Nuannin P. (2006). The Potential of b-value Variations as Earthquake Precursors for Small and Large Events. Digital Comprehensive Summaries of Uppsala Dissertations from the Faculty of Science and Technology.

Richter F.M. (1979). Focal mechanisms and seismic energy release of deep and intermediate earthquakes in the Tonga–Kermadec region and their bearing on the depth extent of mantle flow. *Journal of Geophysical Research,* **84** (B12), 6783–6795.

Riguzzi F., Panza G., Varga P., Doglioni C. (2010). Can Earth's rotation and tidal despinningdrive plate tectonics? *Tectonophysics* **484** (1–4), 60–73.

Shanker D., Kapur N., Singh V.P. (2001). On the spatio temporal distribution of globalseismicity and rotation of the Earth — a review. *Acta Geod. Geophys. Hung,* **36** (2), 175–187.

Sun W. (1992). Seismic energy distribution in latitude and a possible tidal stress explanation. Physics of the Earth and Planetary Interiors, **71** (3–4), 205–216.

Varga P. (1995). Temporal variation of the figure of the Earth and seismic energy release. Publication *of the Institute of Geodesy and Navigation, University FAF, Munich*, pp. 118–127.

Varga P., F. Krumm F., Riguzzi F., Doglioni C., Süle B., Wang K., Panza G.F. (2012). Global pattern of earthquakes and seismic energy distributions: Insights for the mechanisms of plate tectonics. *Techtonophysics*, **530**: 80 – 86.